Available online at www.sciencedirect.com
SCIENCE DIRECT®
Applied Geochemistry 21 (2006) 993–1005
Applied Geochemistry
www.elsevier.com/locate/apgeochem

Spectroscopic investigation on the chemical forms of Cu during the synthesis of zeolite X at low temperature

Roberto Terzano [a,*], Matteo Spagnuolo [a], Luca Medici [b], Fabio Tateo [c], Bart Vekemans [d], Koen Janssens [d], Pacifico Ruggiero [a]

[a] *Dipartimento di Biologia e Chimica Agro-forestale ed Ambientale, Università degli Studi di Bari, Via Amendola 165/A, I-70126 Bari, Italy*
[b] *Istituto di Metodologie per l'Analisi Ambientale (I.M.A.A.), C.N.R, Contrada S. Loja, I-85050 Tito Scalo, Potenza, Italy*
[c] *Istituto di Geoscienze e Georisorse (I.G.G.), C.N.R., Sezione di Padova, c/o Dipartimento di Geologia, Paleontologia e Geofisica, Università degli Studi di Padova, Via Giotto 1, I-35137 Padova, Italy*
[d] *Department of Chemistry, University of Antwerp, Universiteitsplein 1, B-2610, Wilrijk, Belgium*

Received 27 July 2005; accepted 10 March 2006
Editorial handling by M. Hodson
Available online 5 May 2006

Abstract

The direct synthesis of zeolites in polluted soils has proved to be a promising process for the stabilization of metals inside these minerals. Nevertheless, more detailed information about this process is still needed in order to better foresee the fate of metals in treated soils. In this work, zeolite X has been synthesized under alkaline conditions in an aqueous solution containing 2500 mg kg^{-1} of Cu, starting from Na silicate and Al hydroxide at 60 °C. Aluminium, Si and Cu concentrations in the aqueous phase, during zeolite synthesis, were measured over a period of 160 h. The solid products have been characterized over time by XRD, SEM-EDX, ESR, FT-IR, and synchrotron radiation X-ray microbeam absorption near edge structure (μ-XANES) and extended X-ray absorption fine structure (μ-EXAFS) spectroscopy. It appears that the marked reduction of Cu concentration in solution is not only due to a simple precipitation effect, but also to processes connected with the formation of zeolite X which could entrap, inside its porous structure, nano- or micro-occlusions of precipitated Cu hydroxides and/or oxides. In addition, EXAFS observations strengthen the hypothesis of the presence of different Cu phases even at a short-range molecular level and suggest that some of these occlusions could be even bound to the zeolite framework. The results suggest that zeolite formation could be used to reduce the availability of metals in polluted soils.

1. Introduction

The accumulation of metals in soils to levels that are toxic to plants and animals and that can affect the contamination of surface and groundwater has concerned public opinion in many parts of the world. Several remediation technologies have been developed and implemented in recent years to clean up the enormous number of metal contaminated sites that threaten the health of ecosystems. Some of these methods are rapid and very costly (e.g., landfilling or electrolytic treatments), whereas

* Corresponding author. Tel.: +39 80 5442847; fax: +39 80 5442850.
E-mail address: r.terzano@agr.uniba.it (R. Terzano).

0883-2927/$ - see front matter © 2006 Elsevier Ltd. All rights reserved.
doi:10.1016/j.apgeochem.2006.03.004

others are slow but relatively inexpensive (e.g., phytoremediation). The so-called enhanced stabilization/solidification (S/S) technologies (Conner and Hoeffner, 1998; Newton et al., 1999) are particularly interesting, especially considering the combined possibility of immobilizing inorganic contaminants and degrading organic pollutants (Hwang and Batchelor, 2000). Inorganic contaminants are immobilized in situ in such a way that treated soils and sediments can meet regulatory standards for toxicity and leachability, estimated, respectively via bioassays and mild acid extraction tests like the EPA toxicity characteristic leaching procedure – TCLP (Lo et al., 2000). After mixing inorganic salts and silica-based materials such as cement, fly ash, or blast furnace slag, with contaminated soils and sediments under alkaline conditions, various new minerals can be formed (aluminosilicates, Fe and Mn oxides, Fe and Al hydroxides, etc.) that are capable of entrapping significant amounts of inorganic contaminants within their structures, making them unavailable and therefore non-toxic (Conner and Hoeffner, 1998; Phair et al., 2004; Porter et al., 2004; Shi and Spence, 2004).

However, even if many of these technologies are very effective for remediation of soils and sediments contaminated by metals, information on the mechanisms by which metals are immobilized in/on the neo-formed structures and on their catalytic properties is still scanty. It is obvious that the study of metal speciation in extremely complex systems such as remediated soils or sediments is essential in order to assess their long term ecotoxicological impact.

In general, a reduction of metal mobility in soils can be achieved through different mechanisms such as: complexation with organic matter, adsorption on inorganic particles (Fe and Mn oxides, Fe and Al hydroxides, aluminosilicates, etc.), precipitation of discrete mineral compounds and incorporation into neo-formed soil minerals through co-precipitation. Thermodynamically, co-precipitation produces the lowest metal solubility and, therefore, would in principle be the most effective in reducing the bioavailability and toxicity of contaminants (McBride, 1994). The experimental results of Fendorf et al. (1994), Junta and Hochella (1994), and Ford et al. (2001) suggest that the formation of precipitates and co-precipitates is even more important for the reduction of metal availability than previously thought.

Along with amorphous Fe hydroxides (Martínez and McBride, 1998) and Al oxides (Martínez and McBride, 2000), alumino-silicates and in particular zeolites (Mashal et al., 2005; Terzano et al., 2005a) are possible target minerals in which metals could co-precipitate or be trapped. Newton et al. (1999) also have observed that, following the application of a S/S mixture of inorganic constituents containing coal fly ash to a polluted soil, a small amount (not detectable by XRD but only by SEM analysis) of zeolite crystals (mordenite) were formed. The synthesis of zeolites from an aluminosiliceous source like coal fly ash (or any other Si, Al source), added to a polluted soil in a mixture together with other constituents for remediation purposes, could be a promising process which would contribute to the in situ stabilization of metals.

Various zeolites can be synthesized from different source materials and under different hydrothermal conditions. Coal fly ash can be an inexpensive starting material for zeolite synthesis and such an application can partly solve the problem of its disposal (Berkgaut and Singer, 1996; Hollman et al., 1999; Poole et al., 2000; Murayama et al., 2002). The main zeolitic phases usually obtained by hydrothermally treating this material at temperatures ranging from 80 to 150 °C are: sodalite, hydroxysodalite, zeolite X, P, A and Y. The type of zeolite obtained depends on many factors including starting material characteristics, temperature, alkali concentration, reaction time, pressure, and Si/Al molar ratio in the starting solution (Barth-Wirsching and Höller, 1989). Shih and Chang (1996) have reported the low temperature (38 °C) synthesis of zeolite X (zeolite belonging to the Faujasite series) from coal fly ash in 5 days.

Usually, natural or synthetic zeolites are added to polluted soils to reduce metal mobility mainly by acting as highly effective cation exchangers (Gworek, 1992a,b; Shanableh and Karabsheh, 1996; Lin et al., 1998; Moirou et al., 2001; Oste et al., 2002). In previous work the authors have shown that zeolites and in particular zeolite X can be synthesized from fused coal fly ash directly in soil even at 30 °C (Terzano et al., 2005a) and in the presence of high Cu concentrations (Terzano et al., 2005b). In these two papers, the process of zeolite synthesis in soil has also been investigated at 60 °C, in order to simulate, in a shorter period, spontaneous long term transformations of solid phases (Martínez et al., 2001). Such a process was effective in strongly reducing Cu mobility in soil and in stabilizing the metal in the solid phase (Terzano et al., 2005b).

In this context, the key objectives of the present research are: (i) to monitor the synthesis of zeolite X in the presence of Cu, a metal frequently found in agricultural soils that, if present at high concentrations, can become extremely toxic for plants and animals; (ii) to assess whether, and to what extent, the synthesis of zeolite X may lead to a substantial reduction of Cu solubility in the bulk aqueous solution, and (iii) to determine the nature and the chemical form of Cu in/on the newly formed zeolite X by means of several spectroscopic investigations such as Fourier transformed infra-red (FT-IR) spectroscopy, electron spin resonance (ESR) and micro X-ray absorption spectroscopy (μ-XAS: μ-XANES and μ-EXAFS).

In order to more properly study the variations in solubility and the speciation of Cu in the solid phase, without interferences which may typically be posed by other components present in coal fly ash (e.g., Fe oxides, Mn oxides, C residues, etc.) or soil constituents, zeolite X has been synthesized in a Cu-aqueous solution starting from pure Si and Al salts according to the method of Lechert and Kacirek (1991, 1992). However, different from the procedure of Lechert and Kacirek (1991, 1992), in the present research a temperature of reaction of 60 °C instead of 90 °C was adopted for zeolite X synthesis in order to more properly simulate, in a shorter period, long-term processes likely to occur in S/S treated soils (Terzano et al., 2005a). In general, in more complex systems such as treated soils, zeolite X is preferentially synthesised at lower temperatures but in much longer periods (e.g. at 30 °C zeolite X synthesis can occur after 1–3 months Terzano et al., 2005a,b).

2. Materials and methods

2.1. Zeolite X synthesis

Aluminium hydroxide (97.5 g, J.T. Baker) was added to 200 g of a 50% (w/w) NaOH aqueous solution and the mixture was stirred at 100 °C until complete dissolution. The $Al(OH)_3$ solution was cooled at room temperature and 202.5 g of water were added (solution 1). In a separate flask, 13 g of copper acetate (Carlo Erba, ACS) were dissolved in 612 g of water (solution A). Sodium hydroxide (59.12 g) was added to 100 g of solution 1 and mixed until dissolution (solution B). In another flask, 219.7 g of Na silicate solution (Riedel-de Haën) were dissolved by mixing with 612 g of water and 59.12 g of NaOH (solution C). Finally, solution A and solution B were contemporarily and quickly added to solution C and the final solution (solution D) was then stirred for 1 h at room temperature. Copper concentration in the final reaction mixture (solution D) was about 2500 mg kg^{-1}. Immediately at the end of the mixing period (time 0 of the reaction), the mixture was incubated without stirring at 60 °C in an electrical oven for 160 h in a closed polyethylene bottle.

Samples were collected at different time intervals (0, 20, 44, 68, 94, and 160 h) and centrifuged at 20,600*g* for 5 min. The solid phases were then separated and washed 3 times with deionised water and dried at 80 °C for 12 h. Supernatants were collected and analysed by inductively coupled plasma – optical emission spectroscopy (ICP-OES, Thermo Jarrel Ash, Trace Scan) to determine Cu, Si and Al total concentration in solution after zeolite synthesis. All the experiments were conducted in triplicate.

2.2. Solid phase characterization

The solid products were characterized by means of X-ray diffraction (XRD), scanning electron microscopy (SEM) coupled to energy dispersive X-ray (EDX) analysis, electron spin resonance (ESR), Fourier transformed infrared (FT-IR) spectroscopy, synchrotron radiation (SR) X-ray microbeam absorption near edge structure (μ-XANES) spectroscopy and extended X-ray absorption fine structure (μ-EXAFS) spectroscopy.

XRD patterns were collected using a Rigaku D-Max Rapid micro-diffractometer operating at 40 kV and 30 mA with Cu Kα radiation and flat graphite monochromator. The relative amount of zeolite X synthesized was determined using $BaTiO_3$ (Fluka) as an internal standard (Chang and Shih, 1998).

The synthesized crystalline zeolite X samples were mounted by means of a carbon tape on Al stubs, sputter coated with Au and observed with a SEM (LEO Stereoscan 440) operating at an energy of 20 kV and at an intensity of 1 nA. The presence of Cu in the solid phase was confirmed by energy dispersive X-ray analysis.

FT-IR spectroscopy was also used to monitor the process of zeolite synthesis in the presence of Cu. FT-IR measurements were made with a Fourier transform Thermo Nicolet Nexus infrared spectrophotometer using KBr pellets (1 mg of sample in 400 mg of KBr).

ESR spectra were obtained on the dried Cu-zeolite X products collected at various time intervals using a Bruker EPR 200 SRC X-band spectrometer at 9.76 gigahertz (GHz) frequency. The samples were weighed (30 mg) in EPR tubes and the spectra recorded at 100 mW microwave power and 2×1 modulation amplitude. After the original spectra were collected, the powders were exposed to NH_3 vapour (from concentrated NH_4OH in a desiccator) for 24 h and their spectra recorded again. The degree of Cu–NH_3 bond formation provides insight concerning the fraction of Cu atoms that are present at the surface of the Cu-zeolite X product and that can partake in ligand – displacement reactions, thus revealing the structural location of Cu in the aluminosilicatic matrix (McBride, 1982). Moreover, it is well known that Faujasite-type zeolites such as zeolite X are characterized by very large internal cavities (Gottardi and Galli, 1985) that can easily accommodate even quite large complex ions such as $Cu(NH_3)_4^{2+}$.

μ-XANES and μ-EXAFS spectra were collected at 298 K on Beamline L at the Hamburger Synchrotronstrahlungslabor (HASYLAB, Hamburg, Germany). A Si (1 1 1) double-crystal monochromator was used for selection of energy with an energy resolution (ΔE) of ca. 0.8 eV at the Cu–K edge. The beam energy was calibrated by recording the absorption edge from Cu foil in the energy range 8900–9500 eV. The beam was focused down to approximately 20 μm by means of a X-ray Optical Systems (Albany, NY, USA) polycapillary lens. The samples were mixed with BN (Sigma-Aldrich) (1% w/w) and pellets were prepared. The pellets, mounted over slide frames, were placed on a motor x–y–z stage and set at an angle of 45° to the incident beam. μ-XAS spectra were collected in fluorescence-yield mode. For XANES measurements, spectra were collected from 100 eV below to 200 eV above the Cu–K edge in step increments of 1 eV. Typically, 2–3 scans were collected for model compounds and about 10 scans were collected for zeolite X samples. The resulting XANES profiles were evaluated using the WINXAS 3.1 software package (Ressler, 1998). Semiquantitative analysis of the edge spectra was performed by least squares fitting of linear combinations of standard spectra to the spectrum of the sample. XANES spectra of standard Cu compounds such as $CuCl_2$, $Cu(OH)_2$, CuO, $CuSO_4$, Cu_2O, Cu(II)-zeolite X (exchanged), Cu(II)-amorphous alumino-silicate and Cu foil were also recorded.

For EXAFS investigations, spectra of the Cu-zeolite X product collected after 160 h, were acquired from 100 eV below to 600 eV above the Cu–K edge in step increments of 1 eV. EXAFS experimental spectra were used to generate Fourier transforms (FT), which were back transformed to generate Fourier filtered EXAFS spectra (FT^{-1}). The Fourier filtered EXAFS spectra were compared with theoretical EXAFS spectra, calculated by the FEFF-8 program (Ankudinov et al., 1998). Theoretical spectra refer to model compounds, available in the literature, whose structures were determined by X-ray and/or neutron diffraction. The experimental Cu–K edge spectrum obtained for the Cu-zeolite X product was fitted using the structures of various model compounds: CuO (tenorite) (Åsbrink and Norrby, 1970), $Cu(OH)_2$ (spertiniite) (Oswald et al., 1990), $Cu(Cu,Na)[NH_4,O]_8Si_{32}O_{64} \cdot 38H_2O$ (zeolite X) (Vlessidis et al., 1993), $Cu_5[SiO_3]_4(OH)_2$ (shattuckite) (Evans and Mrose, 1977), $Cu_8[Si_4O_{11}]_2(OH)_4 \cdot 0.43H_2O$ (plancheite) (Evans and Mrose, 1977), $CaCuSi_4O_{10}$ (cuprorivaite) (Pabst, 1959), $Cu_6Si_6O_{18}$ (dioptase) (Breuer et al., 1989).

3. Results and discussion

3.1. Zeolite X synthesis

The presence of high concentrations of Cu within the solution from which zeolite X synthesis was occurring, seemed not to significantly hinder the crystallization process. As an example, the XRD pattern of the product obtained by synthesizing zeolite X in 160 h in the presence of a 2500 mg kg^{-1} Cu-solution is reported in Fig. 1. The presence of all the characteristic reflections of zeolite X is clearly visible. Moreover, the formation of no other crystalline phase was detectable. In particular, no XRD detectable Cu crystalline phase was formed during the synthesis process. However, the presence of Cu in/on the solid phase was confirmed by EDX analysis as reported in Fig. 2.

As reported in Fig. 3, zeolite X crystallization started to be detectable after 44 h of incubation at 60 °C and reached almost the maximum degree of crystallization after 68 h. In Fig. 3, the degree of crystallization of zeolite X after 160 h of incubation was considered to be 100%. However, as can be inferred from the non-flat baseline of the diffractogram in Fig. 1, complete crystallization was never achieved and, therefore, an amorphous phase may

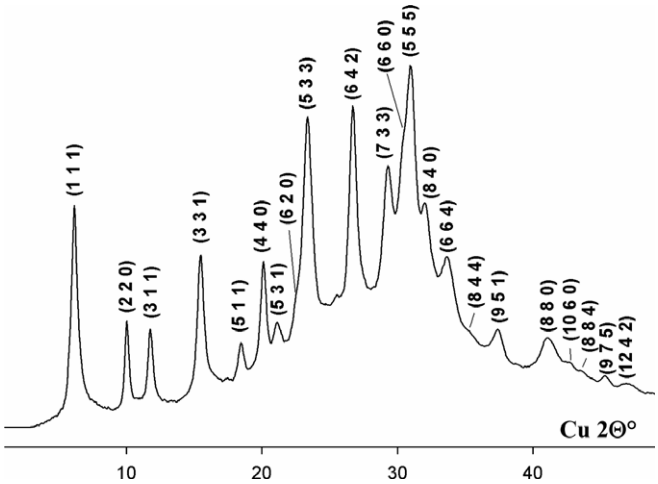

Fig. 1. XRD pattern and typical zeolite X reflections of the solid product obtained by synthesizing zeolite X at 60 °C for 160 h in presence of a 2500 mg kg^{-1} Cu solution.

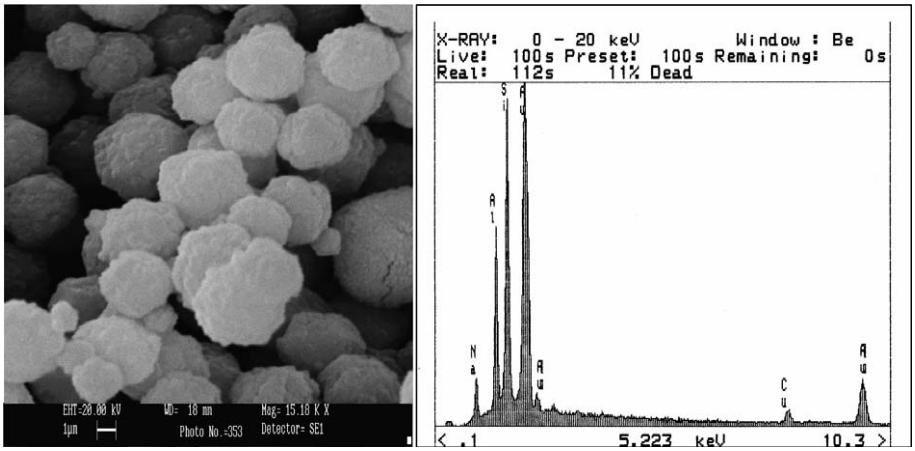

Fig. 2. SEM picture and EDX analysis of the solid product obtained after 160 h by synthesizing zeolite X at 60 °C in presence of a 2500 mg kg^{-1} Cu solution. The sample was coated with a Au layer.

be present in the solid product, owing to the relatively low temperature adopted for zeolite X synthesis.

A marked reduction in Al concentration in solution (by more than 80%) was immediately observed at time 0 (Fig. 3). Afterwards its concentration remained almost constant up to 44 h when it started again to decrease until 94 h. After this period, it reached a value close to zero where it remained until the end of the experiment.

Si concentration was only slightly reduced by about 30% at time 0, then remained almost constant during the whole period under investigation (Fig. 3).

The almost complete depletion of Al from solution confirmed, as reported by other authors (Chang and Shih, 1998), that Al is the controlling species in the formation of faujasites. In fact, according to the literature, Faujasite crystallization starts from Al rich nuclei. Aluminium concentration in solution was immediately and drastically reduced at time 0 and showed a further reduction simultaneously with the beginning of zeolite X crystallization (after 44 h). In addition, the highest amount of zeolite product was achieved when Al species in solution were almost completely depleted. On the other hand, Si concentration, after the initial decrease (time 0), remained quite stable during the whole period of zeolite X synthesis. Moreover, the major fraction of Si added in the starting mixture remained in solution. In fact, according to the data obtained by

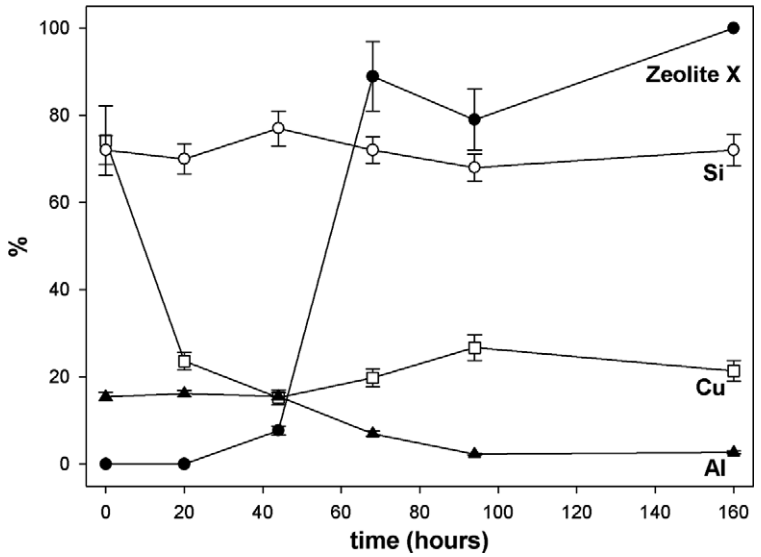

Fig. 3. Trends in zeolite X crystallization and in the relative concentrations (as a % of the initial concentration) of Si, Al and Cu during the process of zeolite X synthesis at 60 °C from Al and Si salts in the presence of dissolved Cu · $[Cu]_i \approx 0.04$ M, $[Si]_i \approx 0.6$ M, $[Al]_i \approx 0.15$ M.

Murayama et al. (2002), a high Si concentration in solution is required during the zeolite crystallization process.

Copper concentration in solution was reduced by almost 30% after 1 h of stirring at room temperature, at the beginning of the incubation period (time 0), to about 1800 mg kg^{-1}, then its concentration was more significantly diminished down to about 600 mg kg^{-1} during the 20 h immediately following the beginning of incubation at 60 °C. Afterwards, this concentration remained almost constant until 160 h. The initial decrease in Cu solubility was mainly due to precipitation phenomena occurring as a consequence of the alkaline salt mixture addition (pH 13). The further reduction observed in the following hours may have been a consequence of other processes occurring during the incubation period and connected with zeolite X condensation and crystallization (see the following sections).

From the reported data it can be calculated that, at the end of the experiment, ca. 8.3 g of Si and 6.75 g of Al were precipitated from the initial solution, corresponding to a final solid phase characterized by a Si/Al molar ratio of 1.2. The theoretical Si/Al molar ratio determined for a zeolite X with the formula $Na_{86}Al_{86}Si_{106}O_{384} \cdot 264\ H_2O$ (Lechert and Kacirek, 1991) is 1.23, very close to the value calculated for the synthesized zeolite X and also to the value determined by EDX analysis. The amount of the solid product recovered at the end of the experiment was 52.3 g, therefore the final concentration of Cu in the solid phase, calculated from the amount of Cu depleted from solution, was about 6.3% (w/w).

3.2. FT-IR

As shown by the FT-IR spectra in Fig. 4, reporting the transformation of the aluminosilicate solid phase precipitated in the presence of Cu, the appearance and disappearance of characteristic bands during the crystallization process was observed. After 68 h the recorded spectra became very similar to each other until the end of the experiment (160 h) and showed characteristic zeolite X bands almost identical to those reported by Flanigen (1976). The appearance of bands at 745, 670, and 560 cm^{-1} and the shift of bands from 1005 to 986 and from 450 to 460 cm^{-1} evidenced the formation of zeolite X. However the occurrence of weak shoulders at 855, 510, and 615 cm^{-1} not reported by Flanigen (1976), but detectable in the samples collected even after 94 and 160 h, suggest the existence of structural defects according to the results of Geidel et al. (1997). Such structural defects can be interpreted as an incomplete crystallization of zeolite X and/or by distortions caused by the presence of occlusions, likely Cu precipitates, in the zeolite structure. However, no evidence of bands ascribed to the presence of significant amounts of Cu precipitates could be detected by the FT-IR measurements, as reported in Fig. 4.

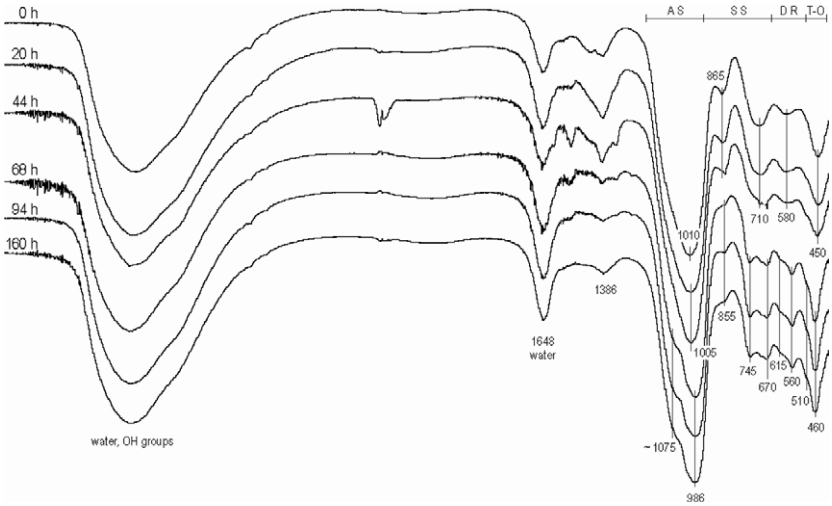

Fig. 4. FT-IR spectra of the solid mixture Cu-aluminosilicate at six stages (0, 20, 44, 68, 94, and 160 h) during zeolite X crystallization process at 60 °C. The bands due to water and OH groups are reported, as well as the typical assignments for zeolites (Flanigen, 1976). AS, asymmetric stretching; SS, symmetric stretching; DR, double ring; T–O, TO4 bending vibration.

3.3. ESR

The chemical form and structural location of Cu in the Cu-zeolite X products was studied by ESR coupled to NH_3 vapour treatment. Fig. 5 shows the behaviour of Cu in the solid phase during the synthesis of zeolite X. Starting from the beginning of the incubation (time 0), it was always possible to observe the typical rigid-limit ESR signal of Cu. This rigid-limit ESR signal was attributed to Cu occupying magnetically isolated sites within or at the surface of the aluminosilicate matrix and indicated reduced movement of the Cu(II) ion due to inner-sphere bonding. However, the ESR signal intensity of Cu in the solid phase decreased significantly after 44 h of incubation, simultaneously with zeolite X crystallization, then reached an almost constant value after 68 h, when about the 90% of zeolite X was already formed. This observation could be attributed to a reduction of adsorption sites for Cu(II) in the aluminosilicate matrix as a consequence of the reduction of the amorphous character of the Cu-aluminosilicate product (and therefore of the surface area) driving Cu out of specific sites into interaction with other Cu ions (Martínez and McBride, 2000). The ESR parameters of the rigid-limit (paramagnetic) Cu were estimated to be $g_{\|} = 2.33$, $g_{\perp} = 2.07$, and $A_{\|} = 140$ gauss and indicated Cu–O bond formation. The hyperfine lines of the $g_{\perp}$ component were not resolvable because of dipolar broadening effects, probably due to Cu(II) ions which were not well dispersed in the aluminosilicatic matrix. The ESR parameters suggested a sixfold coordination of the Cu in an isolated position and excluded the presence of Cu in the tetrahedral zeolite X aluminosilicate framework (Narayana and Kevan, 1983). An underlying broad signal was present in all spectra. The presence of this signal might suggest clustering of Cu atoms leading to shorter distance between neighbouring Cu atoms, and to magnetic interactions (McBride, 1978).

The structural location of Cu in the solid phases was probed using ESR by exposing the samples to NH_3 vapour. Sample treatment with NH_3 molecules displaces superficial Cu that is sorbed (outer sphere complex) or precipitated as $Cu(OH)_2$ or CuO by forming a $Cu(NH_3)_4^{2+}$ complex (McBride, 1982; Martínez and McBride, 1998). As a consequence, an isotropic signal with four hyperfine lines appears, indicating the formation of a rotationally mobile $Cu(NH_3)_4^{2+}$ complex. As reported in Fig. 6, the ESR signal obtained after 24 h of exposure to NH_3 vapour of the Cu-zeolite X product aged for 160 h at 60 °C was nine times more intense than the original signal. However, the shape of the signal obtained as a consequence of the NH_3 treatment was different from the above mentioned isotropic signal. In fact, an asymmetrical signal, similar in appearance to the Cu present in isolated and rigid positions, was obtained. This resulting spectrum was ascribed to $Cu(NH_3)_4^{2+}$ complexes restricted motionally in the framework of zeolite X (Nicula et al., 1965).

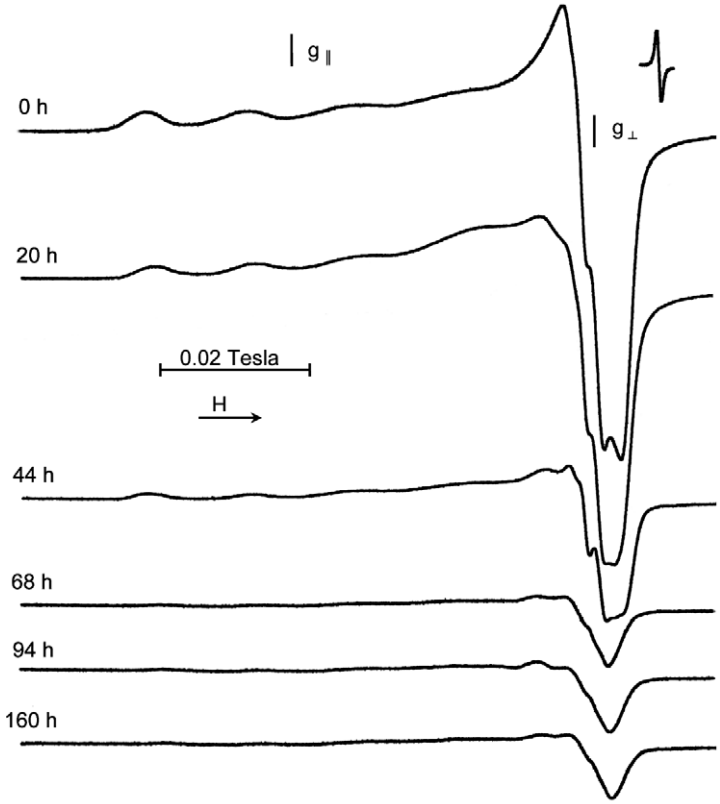

Fig. 5. Cu-ESR spectra of the solid mixture Cu-aluminosilicate at increasing incubation times during zeolite X crystallization process at 60 °C.

However, the shape of the spectrum could be also caused by the interaction of $Cu(NH_3)_4^{2+}$ complex with the external surface of zeolites. In this last case the restriction of the mobility could just be due to the low hydration of the sample. Therefore, the increased signal intensity obtained after NH_3 exposure could be attributed to the presence of separate Cu phases, most probably $Cu(OH)_2$ or CuO which were not observable in the original ESR spectra due to the magnetic interaction of Cu paramagnetic entities. The $Cu(OH)_2$ or CuO precipitates could be located inside the new formed zeolite X as nano- or micro-occlusions as indicated by micro synchrotron radiation X-ray fluorescence (μ-SR-XRF) tomography on zeolite X particles synthesized in soil and hypothesized by Terzano et al. (2005b), and might explain the shape of the ESR spectrum obtained after NH_3 vapour treatment.

3.4. μ-XANES

The chemical state of Cu in and/or on the formed zeolite X was also investigated by means of μ-XANES spectroscopy. The comparison between the linear combinations of Cu standard spectra and the measured XANES spectra for the zeolite X samples allowed an estimation of the concentrations of the possible Cu compounds in the zeolite product to be made. In the zeolite X synthesized after 160 h of incubation at 60 °C, Cu seemed to be mainly present as a mixture of $Cu(OH)_2$ (77%) and CuO (23%). In Fig. 7, an example of the contributions of $Cu(OH)_2$ and CuO to the fitting of the experimental data, is reported. The set of standards used is by no means exhaustive, however these results may be highly indicative of the major forms in which Cu could be present in/on the zeolite mineral. The discrepancies observed in fitting the experimental data may be due to the presence of second neighbour interactions between Cu and Si of the zeolite framework as possibly suggested by μ-EXAFS analyses (see the following section).

Copper hydroxide is the phase that is commonly precipitated from aqueous solutions but, according to Cheah et al. (2000), it is less stable than CuO. However, $Cu(OH)_2$ would become the more stable

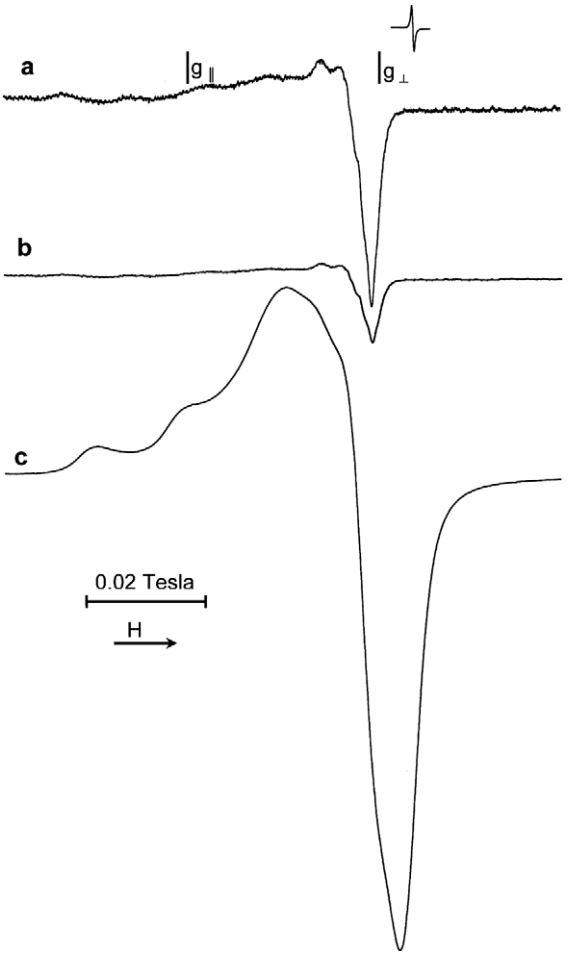

Fig. 6. Effect of NH_3 vapour treatment on the Cu-ESR spectra of the Cu(II)-zeolite X product collected after 160 h of incubation at 60 °C. (a) ESR spectrum of the Cu-zeolite X product; (b) as in (a) but with the same recorded gain of (c); (c) ESR spectrum of the Cu-zeolite X product after 24 h of exposure to NH_3 vapour.

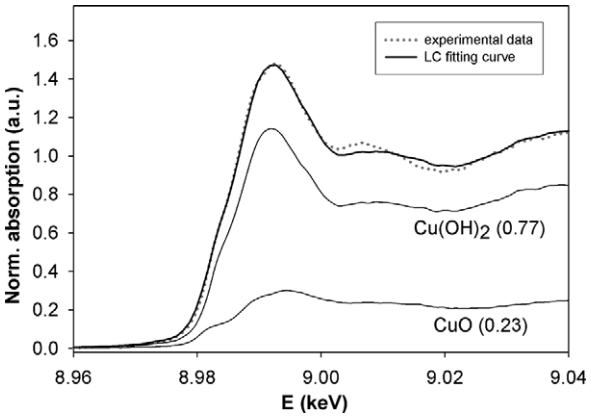

Fig. 7. Experimental data and the least-squares fit for the μ-XANES spectra of zeolite X synthesized at 60 °C in 160 h in presence of Cu. The fractional contribution of the two principal components making up the fitted spectra is also reported.

phase when the precipitating particle sizes are small enough that their surface energy could give an important contribution to the $Cu(OH)_2$ free energy. Usually, with time, the precipitated Cu(II) phases may grow, and $Cu(OH)_2$ converts to CuO.

3.5. μ-EXAFS

The FT and the associated FT^{-1} functions generated from the Cu K-edge EXAFS spectra of zeolite X are reported in Fig. 8. A good match in the peak positions and peak intensities between the experimental spectra of zeolite X and the model compounds was obtained using $Cu_6Si_6O_{18}$ (dioptase), CuO (tenorite), and $Cu(OH)_2$ (spertiniite). In general, some first and second neighbours could be detected, while others could not because of noise interferences. The obtained interatomic distances agreed well with those of the theoretical model compounds.

In $Cu_6Si_6O_{18}$ (Fig. 8a) six paths contributed significantly to the EXAFS; these were O at 1.90 Å, O at 1.92 Å, Cu at 2.91 Å, Si at 3.16 Å, O at 3.85 Å, and O at 4.22 Å (Table 1). The first coordination shell of Cu(II) highlights Cu–O distances at 1.90 and 1.92 Å: the mean of the distances obtained from fitting EXAFS spectrum is only a bit shorter than the theoretical ones (1.91 vs. 1.92 Å). For what concerns the second shell neighbours, a significant contribution to EXAFS frequencies was obtained by Cu atoms at 2.91 Å, corresponding to the equatorial edge-shared Cu atoms, whereas axial edge-shared Cu atoms contributed insignificantly. A Si second-neighbour shell at 3.16 Å could be fitted, despite the presence of three other Si second neighbours around Cu.

In CuO (Fig. 8b) four paths contributed significantly to the EXAFS; these were O at 1.93 Å, Cu at 2.93 Å, Cu at 3.14 Å, and O at 3.81 Å (Table 1). The polyhedron defining the first coordination sphere of Cu is a distorted octahedron defined by O atoms, but only the short bonds of the equatorial ligands (Cu–O: 1.93 Å) contributed significantly to the EXAFS frequencies. Six second neighbour Cu atoms can be fitted: two equatorial edge-shared at 2.93 Å, two axial edge-shared also at 2.93 Å, and, despite their distance from the central atom, two axial edge-shared at 3.14 Å.

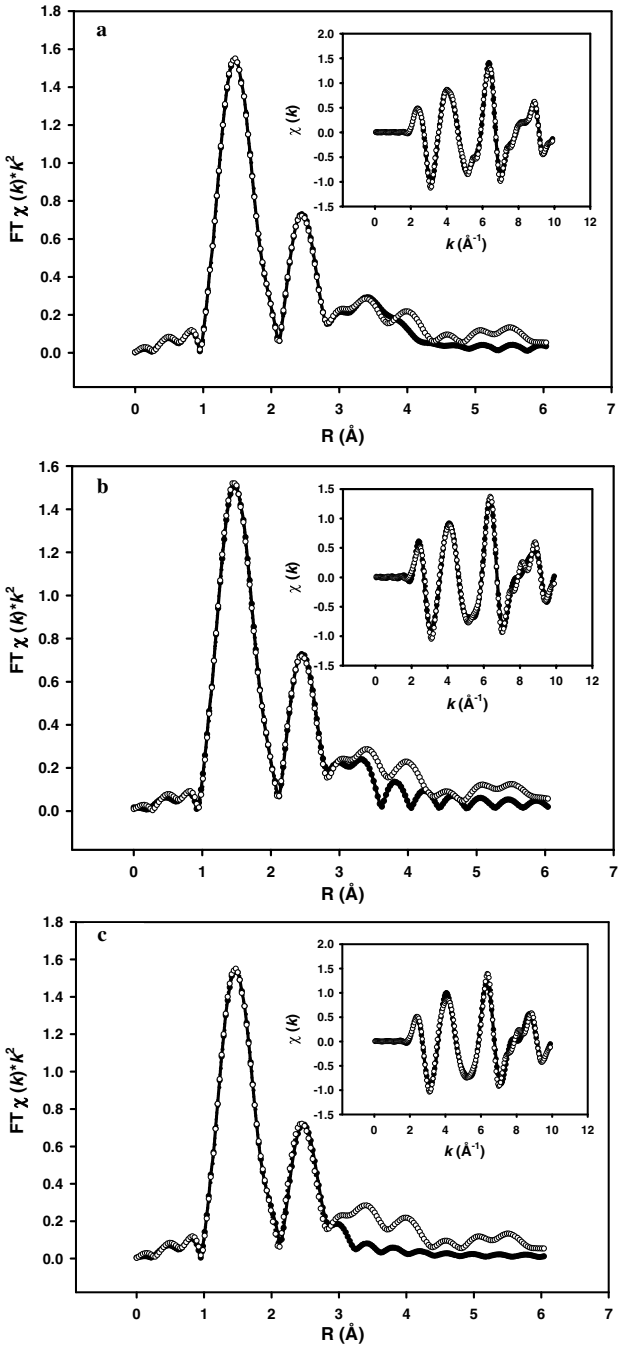

Fig. 8. Cu K-edge EXAFS data for the Cu-zeolite X product synthesized at 60 °C in 160 h. Fourier transform (FT) and associated inverse Fourier-filtered scattering curve (FT^{-1}) spectra (smaller box). Circles indicate experimental data and solid lines indicate the fit curve obtained using: (a) $Cu_6Si_6O_{18}$ (dioptase), (b) CuO (tenorite), and (c) $Cu(OH)_2$ (spertiniite) as reference compounds.

In $Cu(OH)_2$ (Fig. 8c) three paths contributed significantly to the EXAFS; these are O at 1.95 Å, O at 2.41 Å, and Cu at 2.94 Å (Table 1). The significant contributions of the backscattering from the four equatorial O atoms (Cu–O: 1.95 Å) and from an axial O atom (Cu–O: 2.41 Å) suggested that the first coordination shell is defined by an octahedron with 6 oxygen atoms around the Cu central absorber, although the longer axial Cu–O distance could not be fitted. The equatorial edge-shared Cu atom

Table 1
Result of EXAFS analysis

Aa–Sa	*N*	*R* (Å)	σ^2 (Å^2)
$Cu_6Si_6O_{18}$ (dioptase)			
Cu–O	1.8	1.90	0.0054
Cu–O	1.8	1.92	0.0009
Cu–Cu	1.0	2.91	0.0005
Cu–Si	0.7	3.16	0.0049
Cu–O	3.9	3.85	0.0091
Cu–O	5.3	4.22	0.0009
CuO (tenorite)			
Cu–O	3.3	1.93	0.0059
Cu–Cu	4.0	2.93	0.0087
Cu–Cu	1.7	3.14	0.0095
Cu–O	2.4	3.81	0.0005
$Cu(OH)_2$ (spertiniite)			
Cu–O	4.5	1.95	0.0080
Cu–O	0.7	2.41	0.0031
Cu–Cu	2.8	2.94	0.0094

Aa–Sa, relationship between central absorber and scattering atom; *N*, coordination number; *R*, refined interatomic distance; σ^2 (Å^2): Debye–Waller factor.

(Cu–Cu: 2.94 Å) was the only significant contribution of the second shell neighbours, due to its tight link with equatorial O atoms.

EXAFS results suggest that the structural short-range order around Cu in zeolite X is characterized by the presence of different phases. The equatorial Cu–O distances of the first coordination shell range between 1.90 and 1.95 Å, while the axial distances, which are hard to determine (Cheah et al., 2000), are well matched by $Cu(OH)_2$ fit with a Cu–O distance at 2.41 Å; longer axial distances are not revealed; in fact, the $Cu(OH)_2$ fit suggests the presence of phases with Cu 6-coordinated by O atoms, but the characteristic Jahn-Teller distortion of $Cu(O,OH)_6$ octahedra makes it difficult to identify all atoms of the first coordination shell. The second coordination shell is significantly characterized by equatorial edge shared Cu atoms, with a Cu–Cu distance range between 2.91 and 2.94 Å and, to a smaller extent, by Si atoms at 3.16 Å from the absorber, as evidenced by the best fitting of the experimental data obtained with the dioptase model. This last observation, together with the discrepancies observed in fitting μ-XANES data only with a combination of $Cu(OH)_2$ and CuO, could suggest the occurrence of interactions between the microscopic $Cu(OH)_2$ or CuO particles with the structural Si atoms of the zeolite X framework. Probably, more detailed μ-EXAFS measurements using more intense third-generation synchrotron generated X-ray beams could better clarify this aspect of the EXAFS by producing less noisy experimental spectra in the region above 3 Å.

In Cu-exchanged zeolites possessing Faujasite structures such as zeolite X (e.g. zeolite Y), a Cu-O distance ranging from 1.97 to 1.99 Å has been observed (Lamberti et al., 1997), higher than that determined in the present investigation (1.90–1.95 Å). In the same paper, the observed Cu–Cu distance (2.97 Å), also higher than that determined in the present research (2.91–2.94 Å), has been attributed to the presence of Cu–Cu dimers or $(Cu–O–Cu)^{2+}$ oxycations. These differences, together with the much higher pH adopted in the present investigation, confirm that exchange processes could not have taken place during the process of zeolite synthesis in the presence of Cu (exchange is also excluded by the ESR data). Nevertheless, even in the case of exchange processes, it is likely that small amounts of Cu oxides/hydroxides may form on the zeolite surface (Misaelides et al., 1996) or, as small clusters, in zeolite cavities (Grünert et al., 1994; Lamberti et al., 1997).

4. Conclusions

The present paper contains new data on metal stabilization by coprecipitation with amorphous aluminosilicates and subsequent formation of zeolites, a process that may occur during the application of different physico-chemical remediation technologies based on the addition of aluminosilicate materials and alkalizing agents to contaminated soils. According to the data presented in the manuscript, the drastic reduction of metal concentration in solution was not only due to a simple precipitation effect (determined by the high alkaline pH) but also to the formation of a new mineral phase (zeolite X) which could entrap, inside its porous structure, nano- or micro-occlusions of precipitated Cu hydroxides and/or oxides. According to Manceau et al. (2002) occlusions are pockets of "impurity" that are literally trapped inside the growing crystal. The hypothesis of the formation of Cu-precipitate occlusions was supported by the presence of possible small structural defects in zeolite X (as evidenced by FT-IR analysis), by the formation of motionally restricted $Cu(NH_3)_4^{2+}$ complexes reported by ESR analysis, and by the heterogeneous clustered Cu distribution visualized by μ-XRF tomography (Terzano et al., 2005b) on zeolite X particles synthesized directly in a

Cupolluted soil. Moreover, μ-EXAFS investigation strengthened the hypothesis of the presence of different Cu phases even at the short-range molecular level observable with this technique and suggested that some of these occlusions could be even bound to the zeolite aluminosilicate framework.

All the reported findings suggest that zeolite formation in soils could be used as a remediation process to reduce the availability of metals in polluted soils.

Acknowledgements

During the part of this research concerning SR based X-ray microbeam analyses, Roberto Terzano was supported by a European Community Marie Curie Fellowship. The authors thank Gerald Falkenberg (Beamline L, HASYLAB, DESY, Hamburg, Germany) for his precious scientific and technical support in obtaining the experimental data at Beamline L.

References

Ankudinov, A.L., Ravel, B., Rehr, J.J., Conradson, S.D., 1998. Real space multiple scattering calculation and interpretation of X-ray absorption near edge structure. Phys. Rev. B 58, 7565–7576.

Åsbrink, B.S., Norrby, L.-J., 1970. A refinement of the crystal structure of copper(II) oxide with a discussion of some exceptional e.s.d.'s.. Acta Crystallogr. B 26, 8–15.

Barth-Wirsching, U., Höller, H., 1989. Experimental studies on zeolite formation conditions. Eur. J. Miner. 1, 489–506.

Berkgaut, V., Singer, A., 1996. High capacity cation exchanger by hydrothermal zeolitization of coal fly ash. Appl. Clay Sci. 10, 369–378.

Breuer, K.H., Eysel, W., Müller, R., 1989. Structural and chemical-varieties of dioptase, $Cu_6[Si_6O_{18}]\cdot 6\,H_2O$. 2. Structural-properties. Z. Kristall 187, 15–23.

Chang, H.C., Shih, W.H., 1998. A general method for the conversion of fly ash into zeolites as ion exchangers for cesium. Ind. Eng. Chem. Res. 37, 71–78.

Cheah, S.F., Brown Jr., G.E., Parks, G.A., 2000. XAFS study of Cu model compounds and Cu^{2+} sorption products on amorphous SiO_2, γ-Al_2O_3, and anatase. Am. Miner. 85, 118–132.

Conner, J.R., Hoeffner, S.L., 1998. The history of stabilization/solidification technology. Crit. Rev. Envir. Sci. Technol. 28, 325–396.

Evans, H.T., Mrose, M.E., 1977. The crystal chemistry of the hydrous copper silicates, shattuckite and plancheite. Am. Miner. 62, 491–502.

Fendorf, S.E., Lamble, G.M., Stapleton, M.G., Kelley, M.J., Sparks, D.L., 1994. Mechanisms of chromium(III) sorption on silica.1. Cr(III) surface-structure derived by extended X-ray-absorption fine-structure spectroscopy. Environ. Sci. Technol. 28, 284–289.

Flanigen, E.M., 1976. Structural analysis by infrared spectroscopy. In: Rabo, J.A. (Ed.), Zeolite Chemistry and Catalysis, ACS Monographs, vol. 171. American Chemical Society, Washington, DC, pp. 80–117.

Ford, R.G., Scheinost, A.C., Sparks, D.L., 2001. Frontiers in metal sorption/precipitation mechanisms on soil mineral surfaces. In: Sparks, D.L. (Ed.), Advances in Agronomy, vol. 74. Academic Press Inc., San Diego, CA, pp. 41–62.

Geidel, E., Krause, K., Forster, H., Bauer, F., 1997. Vibrational spectra and computer simulations of O-18-labelled NaY zeolites. J. Chem. Soc. Faraday Trans. 93, 1439–1443.

Gottardi, G., Galli, E., 1985. Natural Zeolites. Springer-Verlag, Berlin, pp. 214–222.

Grünert, W., Hayes, N.W., Joyner, R.W., Shpiro, E.S., Rafiq, M., Siddiqui, H., Baeva, G.N., 1994. Structure, chemistry, and activity of Cu-ZSM-5 catalysts for the selective reduction of NO_x, in the presence of oxygen. J. Phys. Chem. 98, 10832–10846.

Gworek, B., 1992a. Inactivation of cadmium in contaminated soils using synthetic zeolites. Environ. Pollut. 75, 269–271.

Gworek, B., 1992b. Lead inactivation in soils by zeolites. Plant Soil 143, 71–74.

Hollman, G.G., Steenbruggen, G., Janssen-Jurkovicova, M., 1999. A two-step process for the synthesis of zeolites from coal fly ash. Fuel 78, 1225–1230.

Hwang, I., Batchelor, B., 2000. Reductive dechlorination of tetrachloroethylene by Fe(II) in cement slurries. Environ. Sci. Technol. 34, 5017–5022.

Junta, J., Hochella, M.F., 1994. Manganese(II) oxidation at mineral surfaces – a microscopic and spectroscopic study. Geochim. Cosmochim. Acta 58, 4985–4999.

Lamberti, C., Spoto, G., Scarano, D., Pazé, C., Salvataggio, M., Bordiga, S., Zecchina, A., Turnes Palomino, G., D'Acapito, F., 1997. Cu^{I}-Y and Cu^{II}-Y zeolites: a XANES, EXAFS and visible–NIR study. Chem. Phys. Lett. 269, 500–508.

Lechert, H., Kacirek, H., 1991. Investigations on the crystallization of X-type zeolites. Zeolites 11, 720–728.

Lechert, H., Kacirek, H., 1992. The kinetics of nucleation of X zeolites. Zeolites 13, 192–200.

Lin, C.-F., Lo, S.-S., Lin, H.-Y., Lee, Y., 1998. Stabilization of cadmium contaminated soils using synthesized zeolite. J. Hazard. Mater. 60, 217–226.

Lo, I.M.C., Tang, C.I., Li, X.D., Poon, C.S., 2000. Leaching and microstructural analysis of cement-based solidified wastes. Environ. Sci. Technol. 34, 5038–5042.

Manceau, A., Marcus, M.A., Tamura, N., 2002. Quantitative speciation of heavy metals in soils and sediments by synchrotron X-ray techniques. In: Fenter, P., Rivers, M., Sturchio, N.C., Sutton, S. (Eds.), Applications of Synchrotron Radiation in Low-Temperature Geochemistry and Environmental Science, Reviews in Mineralogy and Geochemistry, vol. 49. Mineralogical Society of America, Washington, DC, pp. 341–428.

Martínez, C.E., McBride, M.B., 1998. Solubility of Cd, Cu, Pb, and Zn in aged coprecipitates with amorphous iron hydroxides. Environ. Sci. Technol. 32, 743–748.

Martínez, C.E., McBride, M.B., 2000. Aging of coprecipitated Cu in alumina: changes in structural location, chemical form, and solubility. Geochim. Cosmochim. Acta 64, 1729–1736.

Martínez, C.E., Jacobson, A., McBride, M.B., 2001. Thermally induced changes in metal solubility of contaminated soils is

linked to mineral recrystallization and organic matter transformations. Environ. Sci. Technol. 35, 908–916.

Mashal, K., Harsh, J.B., Flury, M., Felmy, A.R., 2005. Analysis of precipitates from reactions of hyperalkaline solutions with soluble silica. Appl. Geochem. 20, 1357–1367.

McBride, M.B., 1978. Retention of Cu^{2+}, Ca^{2+}, Mg^{2+}, and Mn^{2+}, by amorphous alumina. Soil Sci. Soc. Am. J. 42, 27–31.

McBride, M.B., 1982. Hydrolysis and dehydration reactions of exchangeable Cu^{2+} on hectorite. Clay Clay Min. 30, 200–206.

McBride, M.B., 1994. Environmental Chemistry of Soils. Oxford University Press, New York.

Misaelides, P., Godelitsas, A., Kossionidis, S., Manos, G., 1996. Investigation of chemical processes at mineral surfaces using accelerator-based and surface analytical techniques: heavy metal sorption on zeolite crystals. Nucl. Instrum. Methods Phys. Res. Sect. B-Beam Interact. Mater. Atoms 113, 296–299.

Moirou, A., Xenidis, A., Paspaliaris, L., 2001. Stabilization of Pb, Zn, and Cd-contaminated soil by means of natural zeolite. Soil Sediment Contam. 10, 251–267.

Murayama, N., Yamamoto, H., Shibata, J., 2002. Mechanism of zeolite synthesis from coal fly ash by alkali hydrothermal reaction. Int. J. Miner. Process. 64, 1–17.

Narayana, M., Kevan, L., 1983. Tetrahedrally coordinated cupric ion in A-zeolites. J. Phys. C: Solid State Phys. 16, 361–367.

Newton, J.P., Baveye, P., Spagnuolo, M., 1999. Reduction of the bioavailability of PAHs in heavily contaminated soils and sediments via a physico-chemical process. In: Baveye, P., Block, J.-C., Goncharuk, V.V. (Eds.), Bioavailability of Organic Xenobiotics in the Environment. Kluwer Academic Publishers, Dordrecht, The Netherlands, pp. 451–461.

Nicula, A., Stamires, D., Turkevich, J., 1965. Paramagnetic resonance absorption of copper ions in porous crystals. J. Chem. Phys. 42, 3684–3692.

Oste, L.A., Lexmond, T.M., Van Riemsdijk, W.H., 2002. Metal immobilization in soils using synthetic zeolites. J. Environ. Qual. 31, 813–821.

Oswald, B.H.R., Reller, A., Schmalle, H.W., Dubler, E., 1990. Structure of copper(II) hydroxide, $Cu(OH)_2$. Acta Crystallogr. C 46, 2279–2284.

Pabst, A., 1959. Structures of some tetragonal sheet silicates. Acta Crystallogr. 12, 733–739.

Phair, J.W., van Deventer, J.S.J., Smith, J.D., 2004. Effect of Al source and alkali activation on Pb and Cu immobilisation in fly ash based ''geopolymers''. Appl. Geochem. 19, 423–434.

Poole, C., Prijatama, H., Rice, N.M., 2000. Synthesis of zeolite adsorbents by hydrothermal treatment of PFA wastes: a comparative study. Miner. Eng. 13, 831–842.

Porter, S.K., Scheckel, K.G., Impellitteri, C.A., Ryan, J.A., 2004. Toxic metals in the environment: thermodynamic considerations for possible immobilization strategies for Pb, Cd, As, and Hg. Crit. Rev. Envir. Sci. Technol. 34, 495–604.

Ressler, T., 1998. WinXAS: A XAS Data Analysis Program under MS Windows. J. Synch. Rad. 5, 118–122.

Shanableh, A., Karabsheh, A., 1996. Stabilization of Cd, Ni and Pb in soil using natural zeolite. J. Hazard. Mater. 45, 207–217.

Shi, C., Spence, R., 2004. Designing of cement-based formula for Solidification/Stabilization of hazardous, radioactive, and mixed wastes. Crit. Rev. Envir. Sci. Technol. 34, 391–417.

Shih, W.H., Chang, H.L., 1996. Conversion of fly ash into zeolites for ion-exchange applications. Mater. Lett. 28, 263–268.

Terzano, R., Spagnuolo, M., Medici, L., Tateo, F., Ruggiero, P., 2005a. Zeolite synthesis from pre-treated coal fly ash in presence of soil as a tool for soil remediation. Appl. Clay Sci. 29, 99–110.

Terzano, R., Spagnuolo, M., Medici, L., Vekemans, B., Vincze, L., Janssens, K., Ruggiero, P., 2005b. Copper stabilization by zeolite synthesis in polluted soils treated with coal fly ash. Environ. Sci. Technol. 39, 6280–6287.

Vlessidis, A.G., Evmiridis, N.P., Beagley, B., Armitage, D.N., 1993. Cupramine ion-exchanged NaX zeolite and crystal-structure analysis. Z. Kristall. 203, 17–27.